Myostain is Involved in GINSENOSIDE-Rb1-mediated anti-obesity

Hong-Shi Li
Shandong University Qilu Hospital
Jiang-Ying Kuang
The Second Hospital of Shandong University
Gui-Jun Liu
Shandong University School of Medicine: Shandong University Cheeloo College of Medicine
Wei-Jie Wu
Shandong University Qilu Hospital
Xian-Lun Yin
Shandong University Qilu Hospital
Hao-Dong Li
Shandong University School of Medicine: Shandong University Cheeloo College of Medicine
Lei Wang
Shandong University Qilu Hospital
Wen-jiang Yan
Shandong University Qilu Hospital
Tao Qin
Shandong University Qilu Hospital
Wen-Cheng Zhang
Shandong University Qilu Hospital
Xiao-Ting Lu
Shandong University Qilu Hospital
Yuan-Yuan Sun (syy912@126.com)
Shandong University Qilu Hospital https://orcid.org/0000-0001-8671-5522

Research

Keywords: Ginsenoside Rb1, Obesity, MSTN, Fndc5,UCP-1

Posted Date: November 19th, 2021

DOI: https://doi.org/10.21203/rs.3.rs-1019424/v1

Abstract

Obesity, as one of the major public health problems in the world, has attracted more and more attention. Rb1 is the most abundant active component of Panax ginseng and it has been reported to have benefit effects on obesity and diabetes. But the mechanisms of Rb1 in regulation of obesity are not very clear. In this study, by use of obese mice, we found that Rb1 not only reduced body weight but also decreased myostain (MSTN) expression,which plays a vital part in the regulation of obesity. In vitro, we found that Rb1 treatment also decreased MSTN expression in differentiated C2C12 cells (Myoblast cells) and 3T3-L1 cells (adipocytes). Fndc5, as the downstream of MSTN, was increased after Rb1 treatment.

Conclusions

Our results showed that Rb1 may ameliorate obesity in part through MSTN/Fndc5 signaling pathway. Our study provides important experimental evidences for the treatment of obesity by Rb1.

Introduction

Obesity, as one of the main public health problems in the world, can leading to dyslipidemia, insulin resistance, type 2 diabetes, hypertension, heart failure, tumors, and obstructive sleep apnea (OSA). The main characteristic of obesity is the large accumulation of triglycerides (TG) in adipose tissue, which due to adipocyte hyperplasia (increased number) or hypertrophy (increased size) or even both. It was believed that adipocyte hypertrophy occured before adipocyte hyperplasia and was the major mechanism of fat mass expansion (Faust et al., 1978) (Duncan et al., 2007). Adipose tissue is mainly composed of fat cells, including white fat, brown fat as well as beige fat. When the body's energy intake far exceeds the amount consumed, the excess part will be stored as white fat. Treatment of obesity is an effective way to prevent a variety of diseases.

Ginseng, as one of traditional Chinese medicine, has been found and used for thousands of years in Eastern Asia. It has been revealed that Rb1, the most abundant bioactive component of Panax ginseng, can improve leptin sensitivity (Wu et al., 2018), ameliorate glycolipid metabolism (Shang et al., 2008), reduce triglyceride accumulation (Park et al., 2008) and reduce fatty liver (Shen et al., 2013). Although aquaporin 7 (Guo et al., 2020), AMPK (Shen et al., 2013). PI3K/Akt signaling pathway (Chen et al., 2016) and PPARγ (Song et al., 2020) have been reported to be included in the effects of Rb1 on adipocytes and adipose tissue, the mechanisms of Rb1 in regulating body weight are still unclear.

Myostatin (MSTN; also called GDF8) is a member of the transforming growth factor β (TGFβ) superfamily. It is predominantly secreted by skeletal muscle. The high expression of MSTN can inhibit muscle growth and development (McPherron et al., 1997). Studies have shown that there was increased muscle mass, reduced fat deposition, improved insulin sensitivity, enhanced fatty acid oxidation, and promoted resistance to obesity in MSTN knock out mice. (Bernardo et al., 2010; Lebrasseur, 2012; Zhang et al., 2012). It was found that there is higher expression of MSTN in adult skeletal muscle and lower expression level in adult adipose tissue. Type 2 diabetes mellitus patients showed significantly lower

MSTN levels and higher irisin levels than controls (Garcia-Fontana et al., 2016). Deletion of MSTN prevents the age-related increasement of adipose tissue mass and partially improved the obese and diabetic phenotypes in mice (McPherron and Lee, 2002). In human and mouse models, the higher levels of MSTN in muscle have been found to be positively related to obesity, Type1 and Type2 diabetes (Milan et al., 2004). Previously, researchers discovered that plasma and muscle MSTN protein levels increased with both body mass and the severity of insulin resistance in extremely obese and lean human subjects (Hittel et al., 2009). In myoblasts, MSTN mediated myostatin signal by specifically inducing Smad3 phosphorylation and interfering with the activity and expression of myoblast differentiation factor MyoD, hence the inhibition of the differentiation of myoblasts into myotubes (Langley et al., 2002). In vitro, recombinant MSTN predominantly promoted the proliferation of 3T3-L1 preadipocytes and reduced lipid accumulation in 3T3-L1 cells consequently by inhibiting the expression of critical lipogenic enzymes and promoting lipolytic enzymes to express (Langley et al., 2002). However whether MSTN is involved in weight loss caused by Rb1 has not been reported.

Methods

Animals

We fed forty C57BL/6 male mice (Six-week old) on high-fat diet (HFD) for 12 weeks. Then these mice were divided into two groups when body weight arrived about 55g: the control (CTR) group (intraperitoneally (ip) administered with saline), the Rb1 group (ip administered with Rb1, 14 mg/kg/d). Body weight was monitored every day. Mice fed a normal diet were randomly divided into 2 subgroups: the Chow group (fed a normal diet and treated with saline) and Chow+Rb1 group (fed a normal diet and treated with Rb1). The body weight was measured weekly. Mice were housed on a 12-h light/dark cycle. All animal protocols were approved by the Institutional Animal Care and Use Committee of Cheeloo College of Medicine, Shandong University (animal ethics number is KYLL-2018 (KJ) A-0072).

RNA-seq library generation and analysis

Total RNA was extracted through RNeasy mini kit (Qiagen, Germany). With the guidance of TruSeq™ RNA sample preparation guide, paired-end libraries were synthesized by the use of TruSeq™ RNA Sample Preparation kit (Illumina, USA). The products were then purified and concentrated by PCR to produce the final cDNA library which were then quantified by Qubit® 2.0 Fluorometer (Life Technologies, USA) and verified by Agilent 2100 bioanalyzer (Agilent Technologies, USA) to calculate the mole concentration and confirm the insert size. With the library diluted to 10 pM, cluster was generated by cBot and then sequenced on the Illumina NovaSeq 6000 (illumina, USA). The differentially expression of genes was identified with both the P value < 0.05 and a fold-change of >1.5 between the two groups.

Serum measurements

Serum total cholesterol, triglyceride, low density lipoprotein-cholesterol, high density lipoprotein-cholesterol, serum creatinine and glutamic-oxalacetic transaminease were detected by assay Kits

(Changchun Huili Biotechnology Co., Ltd).

Metabolic cage

The O_2 consumption (VO_2), CO_2 production (VCO_2) and heat were detected by using a Oxymax/CLAMS animal metabolic system (Coulumbus Instruments). Experiments involved CTR and Rb1 treated mice at 20-22 weeks old. Mice were monitored for 48h individually and data were collected per 30 minutes after 24 hours adaption.

Intraperitoneal glucose tolerance test

On the 16th week, the intraperitoneal glucose tolerance test (IPGTT) was conducted. Mice were fasting overnight in advance and then intraperitoneally injected with glucose at a dose of 2 g/kg body weight. Glucose concentrations in blood taken from the tail vein of the mice were measured respectively at 0 (fasting), 15, 30, 60 and 120 min after glucose administration.

C2C12 cell culture and treatment

C2C12 murine myoblasts were bought from American Type Culture Collection (Manassas, VA, USA) and were cultured in Dulbecco's Modified Eagles Medium (DMEM) with 10% fetal bovine serum (FBS), 100 IU/mL streptomycin, and 100 IU/mL penicillin. Differentiation medium was made up of DMEM medium which contained 2% horse serum. When cell's confluence reaching 90%, the medium was changed to differentiation medium to induce differentiation of C2C12 cell. Skeletal muscle differentiation from C2C12 cells was induced in differentiation medium for 5-8 days (Baek et al., 2019). Then Rb1 (0, 10μM, 20μM, 40μM) was added into differentiated cells. After stimulation for 24hours, cells were harvested.

3T3-L1 cell culture and treatment

3T3-L1 preadipocytes of mouse were bought from American Type Culture Collection (ATCC, US) and were cultured in high glucose DMEM containing 10% FBS in a saturated humidity atmosphere of 5% CO_2 at 37°C. The 3T3-L1 preadipocyte differentiation was used the classic cocktail method. Briefly, cells were treated with a mixture of 1μM dexamethasone, 10 μg/mL insulin and 0.5 mM 3-isobutyl-1-methylxanthine in DMEM for 2 days. Then the medium was replaced by DMEM containing 10% FBS and 10μg/mL insulin. After that, the cells were cultured 2 more days, and the growth medium used for an additional day composed of DMEM with 10% FBS. When there were accumulated lipid droplets in the cytoplasm in more than 90% of the 3T3-L1 cells, they could be further studied. The dose of Rb1 was 0, 20μM and 40μM (Guo, R. et al, 2020). After stimulation for 24hours, cells were harvested.

For cells with MSTN overexpression, 3T3-L1 induced adipocytes were divided into four groups: CTR+vehicle (C+V), Rb1+vehicle (R+V), Rb1+MSTN (Gene ID:17700) (R+M), MSTN overexpression group (M). In C+V group, control adenovirus (ADV) was added into cells. In R+V group, 40μM Rb1 and control ADV were added into cells. In R+M group, 40μM Rb1 and MSTN-ADV were added into cells. In M group,

MSTN-ADV were added into cells.Rb1 was added to cells 24 hours after viral transfection. The multiplicity of infection (MOI) was 50. After 24 hours, cells were harvested.

Oil red O staining

Oil red O staining was used to detect the lipid droplets in the cytoplasm of 3T3-L1 induced adipocytes. Cells were placed on cover slides in plates and transfected with vehicle and adenovirus conjuncted with MSTN (OBiO Scientific service). After 24hours, Rb1 was added into cells. 24hours later, cells were washed with PBS two times and fixed with 4% paraformaldehyde for 15min at room temperature. Then cells were washed with PBS for three times and 0.5% oil red O was added to the cells and incubated for 1hour. After three times of PBS wash, cells were observed under a microscope at 100× magnification. To quantify cellular lipid, stained cells were eluted with 100% isopropanol and incubated for 10 min. Then 150ul lysate was added into 96 - well plates. Absorbance was determined at 500 nm with full wavelength detector (SpectraMax M5/M5e, Molecular Devices).

RT-PCR

Real-time PCR system detects mRNA expression. Total RNA was extracted from peritoneal macrophages by TRIzol reagent (Life Technologies). For reverse transcription (RT), a PrimeScript RT reagent Kit (Takara, Shiga, Japan) worked. As described previously, quantitative PCR was performed using SYBR Premix Ex Taq (Takara) and a Roche Light Cycler 480 II instrument in a 96-well plate following the manufacturer's protocol. The primers below were used to amplify MSTN, Fndc5 and Actin. MSTN-F: TCACGCTACCACGGAAACAA; MSTN-R: AGGAGTCTTGACGGGTCTGA. FNDC5-F: TCATGTGGGCAGGTGTTATAG; FNDC5-R: TGTTATTGGGCTCGTTGTCCT. Actin-F: CCACACCCGCCACCAGTTCG, Actin-R: TACAGCCCGGGGAGCATCGT.

Western blotting

RIPA lysis buffer supplemented with a complete protease inhibitor cocktail was used to lyse cells and tissues on ice. Protein of equal amounts (10 μg) were separated with a 10% SDS-PAGE gel. Then it was transferred to PVDF membranes (0.22 μm, Millipore). Membranes were obstructed in 5% skim milk powder and incubated with primary antibodies against MSTN (AF788; R&D Systems), Fndc5 (ab131390; Abcam), alpha tubulin (11224-1-AP, Proteintech) was used as CTR.

Histopathological staining

The subcutaneous fat, epididymis fat, brown fat and skeletal muscle were taken immediately. One half of tissues were fixed in 4% formaldehyde overnight. The other half of tissues were frozen at -80 ° C for molecular experiments. Tissues embedded in paraffin were cut into serial 5 μm cross-sections. After they were dewaxed, subcutaneous fat, epididymis fat and brown fat sections were stained with hematoxylin and eosin (H&E). Size of adipocyte was determined by measurement of cell diameter. Immunohistochemical staining was performed with MSTN antibody (AF788; R&D Systems; 1:100). The secondary antibody was Rabbit Anti-Goat IgG(H+L), HRP conjugated (SA00001-4, Proteintech;1:200).

Livers were frozen in OCT embedding medium and then stained the10-μm sections with Oil-red O. The sections were taken photographs by a whole slide imaging scanner (Pannoramic SCAN II 3D HISTECH).

ELISA assay

The MSTN in serum, culture supernatant of differentiated C2C12 cells and 3T3-L1 cells were determined via ELISA kits (MSTN, TAE-626m, Tianjin Anoric Biotechnology Co., Ltd) according to the manufacturer's protocol. Plates were read on a spectrometer at 450 nm wavelength after the procedure. The results were converted to numeric values by using standard curves.

Statistical analysis

SPSS 19.0 (SPSS Inc., Chicago, IL) was used in this article. All data are represented as mean ± SEM. Use Student's t test to determine comparison between two groups and one-way ANOVA with Tukey's post-hoc test to determine multiple groups . Consider $P < 0.05$ as statistically significant.

Results

1. Rb1 decreased body weight, cholesterol and triglyceride in obese mice

To investigate how Rb1 affected body weight in obese mice, a mouse model of obesity was established through HFD feeding. After HFD feeding for 12 weeks, the body weight of the mice was dramatically increased. We divided the mice into two groups: the CTR group and the Rb1 group. After Rb1 injected, the body weight was detected every day. Results showed that the body weight of obese mice was predominantly reduced by Rb1 treatment from 7 days after Rb1 injected (Fig1A). The liver function and kidney function was not affected by Rb1 injection (Fig1B-C). Serum total cholesterol and total triglyceride showed decreased expression in Rb1 treated mice. There was no significant differences in CTR group and Rb1 group by high density lipoprotein cholesterol and low density lipoprotein cholesterol (Fig1D). Mice treated with Rb1 became significantly thinner (Fig1E).

2. Rb1 improved the glucose tolerance and increased basic metabolic activity in obese mice

Obesity is tightly connected with insulin resistance and glucose intolerance. In compared with HFD-fed CTR mice, Rb1 group mice showed improved glucose intolerance (Fig2A).

We also evaluated the effect of Rb1 on basic metabolic activity. In the conditions of HFD feeding, mice in Rb1 group showed increased oxygen consumption, carbon dioxide production and heat production (Fig2B-D). The increased resting metabolic rate might explain the decreased body weight seen in mice injected with Rb1.

3. Rb1 improved adipocyte hypertrophy and fatty liver in obese mice

A decrease in adipose tissue mass can be ascribed to a decrease in adipocyte number or size on account of abnormal differentiation, or both. To reveal the mechanism of decreased adiposity in Rb1 treated mice,

we measured the adipocyte size and weight in adipose tissue of CTR and Rb1 treated mice. There were decreased epididymis white adipose tissue （epiWAT） and subcutaneous white adipose tissue（ingWAT） weight in Rb1 treated mice (Fig3A-F). H&E staining indicated smaller adipocytes in both ingWAT, epiWAT and BAT of Rb1 treated mice than CTR mice (Fig3G-J). Because of the close association between hepatic steatosis and obesity, insulin resistance, we took the effect of Rb1 on hepatic lipid deposition into assessment. Results showed that there was alleviated fatty liver in Rb1 treated mice (Supplemental Fig1 D).

4. Rb1 decreased MSTN mRNA and protein expression in adipose tissue , skeletal muscle and serum

To explore the specific mechanism of how Rb1 caused the reduction of adipocyte hypertrophy, we used gene array assay of adipocyte tissues from CTR and Rb1 treated mice. In Rb1 treated mice, the expression of adipogenic transcription factor such as CCAAT/enhancer-binding protein β (C/EBPβ) was decreased. The MSTN was dramatically decreased in adipose tissue in Rb1 treated mice (Fig4A). Results also showed that Rb1 is involved in many biological processes, such as lipid metabolism, energy metabolism etc (Fig4B). We further detected the protein level of MSTN in subWAT, consistent with the results found in mRNA level, the MSTN protein level was decreased in Rb1 group (Fig4C and D). The MSTN in serum was also detected by ELISA, results showed that there was decreased MSTN in Rb1 treated mouse serum (Fig4F). The importance of MSTN in obese mice has been deeply studied, Rb1 improved obese mice may through MSTN. As a molecular in the downstream of MSTN, Fndc5 also play an important role in obesity and diabetes. We found a higher expression of Fndc5 expression in adipocyte tissue (Fig4C and E). Immunohistochemical staining of adipose tissue and skeletal muscle showed that there was decreased expression of MSTN in Rb1 treated mice (Fig4G and H). WB analysis also showed the increased expression of FNDC5 and decreased expression of MSTN in skeletal muscle (Fig4I). BAT is characterized by the expression of UCP1, and the expression quantity of UCP1 represents the volume of BAT. Our results showed that Rb1 promoted UCP1 expression in white adipocyte tissue, thus promoted browning of white fat (Supplemental Fig1C).

5. Rb1 decreased MSTN mRNA and protein expression in differentiated C2C12 myoblasts and 3T3-L1 adipocytes

In order to further study the effect of Rb1 in obesity, we cultured C2C12 cells and 3T3-L1 cells in vitro with and without Rb1 treatment respectively. Differentiated C2C12 myoblasts expressed MYH4 in our study, we found a high expression of MYH4 in C2C12 cells induced myoblasts (Fig5C). Differentiated 3T3-L1 adipocytes and C2C12 cells were treated with Rb1 at different concentrations for 24h. The results showed that the MSTN mRNA was decreased in the condition of 20 to 40 μM Rb1 and the Fndc5 mRNA was increased under treatment with 40 μM Rb1 in differentiated C2C12 cells (Fig5A-B). The Fndc5 protein level was upregulated when treated with 10 to 40 μM Rb1 and the level of MSTN protein was downregulated by the treatment of Rb1 from 10 to 40 μM Rb1 in differentiated C2C12 cells (Fig5C-E).

In differentiated 3T3-L1 adipocytes, 20 μM and 40 μM Rb1 decreased MSTN mRNA expression and 40 μM Rb1 increased Fndc5 mRNA expression (Fig5F-G). In protein level, 20 μM and 40 μM Rb1 significantly

increased Fndc5 expression and decreased MSTN expression (Fig5H-J).

We also detected the MSTN protein level in C2C12 cell and 3T3-L1 cell culture supernatant. Our results showed that there was decreased MSTN in Rb1 treated cells (Fig5K-L).

6. Rb1 inhibited lipid deposit through MSTN in 3T3-L1 induced adipocytes

In order to further study the mechanism of Rb1 in regulating lipid deposit, MSTN was overexpressed in 3T3-L1 induced adipocytes. WB showed that Rb1 decreased MSTN expression and increased Fndc5 expression. But MSTN overexpression counteracts the effect of Rb1 (Fig6 A-C). Oil red O stain showed that Rb1 decreased lipidosis but this effect was offseted by the overexpression of MSTN (Fig6 D-E).

Discussion

In this research, we explored the role of Rb1 on obesity and relevent metabolic disturbances in mice. The results showed that Rb1 treatment reduced body weight and adipocyte enlargement and increased resting metabolic rate in HFD-induced obese C57BL/6 mice. Rb1 treatment decreased MSTN in adipose tissue, skeletal muscle and serum in vivo. In vitro, Rb1 treatment decreased MSTN mRNA and protein expression in differentiated C2C12 cells and 3T3-L1 cells. We also found that Rb1 treatment promote Fndc5 mRNA and protein expression. MSTN overexpression counteracted the effect of Rb1 in inhibiting lipid deposition in 3T3-L1 cells. These results indicated that MSTN/Fndc5 signaling pathway was involved in Rb1 ameliorating obesity status.

Under the influence of environmental and genetic factors, obesity has association with energy-balance dysregulation (Kopelman, 2000). The biological characteristics of obesity are adipocyte hypertrophy and excessive adipose accumulation. The maintenance of lipid homeostasis depends on lipolysis and lipogenesis in adipocytes. Adipose tissue, as an important energy storage organ, has become a therapeutic target for obesity. Brown adipose tissue plays an important role in promoting total energy consumption in regulating the body's energy metabolism by producing heat (Algire et al., 2013). It is more interesting that brown adipose tissue has the ability to protect from obesity by releasing batokines, clearing triglycerides, and reducing insulin resistance (Jeremic et al., 2017). Browning of white fat helps to restrict obesity and obesity-related disorders. Though the most common factor for fat browning has been exercise, there may be other factors for example, Rb1 that involved. In our study, we found smaller adipocyte diameter and increased basic metabolic activity in Rb1 treated mice.

Ginseng, as the root of the Panax ginseng, has been believed to prolong life and resist aging. Ginsenosides are the most important bioactive components of ginseng. Studies have shown that there are multiple benefits of ginsenosides in circulatory, immune, endocrine and central nervous systems (Kim, 2018). Rb1, as the richest and most representative ginsenoside, has been reported to influence both obesity and diabetes. For example, Min Liu, et al found that Rb1 significantly reduced food intake, weight growth, and body fat content, increased energy expenditure and improved glucose tolerance in HFD-induced obese mice. The mechanism involved was that Rb1 activated the phosphatidylinositol 3-

kinase/Akt signaling pathway and inhibited NPY gene expression in the hypothalamus(Chen et al.,2016). Lei Wang et al found that Rb1 could markedly diminish the mouse body weights of HFD-induced obesity and the mechanism involved was that Rb1 enhanced AQP7 expression both in vivo and in vitro. AQP7 take part in the process of the transport of triglycerides and adipogenesis in adipocytes (Hibuse et al., 2006). The expression level of AQP7 is closely associated with the occurrence of obesity and type 2 diabetes (Prudente et al., 2007). In Ye Xiong et al study, they found that Rb1 suppressed food intake, body weight gain, body fat content and increased energy expenditure through stimulating c-Fos expression in brain areas and activating the phosphatidylinositol 3-kinase/Akt signaling pathway and inhibited NPY gene expression in the hypothalamus (Xiong et al., 2010). In Seona Lim et al study, they found that Rb1 promoted browning of white fat through beta 3 adrenergic receptor activation and increased expression of UCP-1(Lim et al., 2019). In Shen ling et al study, they found that Rb1 ameliorated fatty liver by activating AMP-activated protein kinase in obese rats (Shen et al., 2013).

In our study, we found that Rb1 decreased body weight, cholesterol, triglycerides and body fat contant in obese mice. Oil red O staining showed that the lipid in liver in Rb1 treated mice was significantly decreased. Rb1 improved glucose tolerance and increased basic metabolic activity. Our results are consistent with those of published studies. Changes in food intake in mice treated with Rb1 are still controversial. Some studies have found that Rb1 reduces food intake (Xiong et al., 2010), while others have found that Rb1 does not affect food intake (Shin and Yoon, 2018). In our study, we found that there was a decrease in food intake in Rb1 treated mice, but the difference was not statistically significant(Supplementary Fig1B). Some studies have found that Rb1 promotes adiogenesis. For example, in Wenbin Shang et al study, they found that Rb1 promoted adiogenesis in 3T3-L1 cells and the mechanism involved the enhancement expression of PPARgamma and C/EBPalpha (Shang et al., 2007). In L-S Chan et al study, they also found that Rb1-promoted adipogenesis with PPARγ binding and miR-27b regulation (Chan et al., 2012). In the above studies, Rb1 was used to stimulate 3T3-L1 cells, then cells were induced to transform into adipocytes. In this process, Rb1 promoted adiogenesis in 3T3-L1 cells. But in our study, we first induced 3T3-L1 cells to become adipocytes, and then stimulated the cells with Rb1 to observe the effect, and finally found that Rb1 can reduce lipid deposition in adipocytes. In our study, we found that Rb1 can reduce lipid deposition in 3T3-L1 induced adipocytes, which was consistent with previous research. In Lim S, et al study, they also found that Rb1 induced lipolysis in 3T3-L1 adipocytes (Lim et al., 2019). But some studies have also reported that ginseng extract can inhibit lipodysis. Hong Wang et al found that ginseng extract inhibited lipolysis by activating PDE4 in rat adipocytes (Wang et al., 2006). In Wenbin Shang et al study, they found that Rb1 at a concentration of 10μM can inhibit lipolysis in 3T3-L1 adipocytes (Yu et al., 2015). In our study, we found that a concentration of 40μM Rb1 significantly decreased lipidosis in 3T3-L1 adipocytes. The difference in our studies may be due to the dose of Rb1 applied.

By use of gene array assay of the control and Rb1 treatment mouse adipose tissues, we found that the expression of MSTN was significantly decreased. This is a new finding which has not been reported in previous studies . Further study also found decreased expression of MSTN protein level in skeletal muscle, adipose tissue and serum. Overexpression of MSTN in Rb1 treated 3T3-L1 induced adipocytes

counteracted the effect of Rb1 in inhibiting lipidosis (Fig6A-E). The traditional view is that MSTN only acts as a negative factor for skeletal muscle growth and plays an vital part in inhibiting skeletal muscle growth(McPherron and Lee, 1997). Recent researches have shown that MSTN expresses not only in skeletal muscle, but also widely in mammalian adipose tissue, breast, heart tissue, lymphatic tissue and other tissues(Lyons et al., 2010). In 3T3-L1 preadipocytes, MSTN mainly inhibits fat production. In the process of differentiation, 3T3-L1 preadipocytes treated with MSTN significantly inhibited adipogenesis by regulating PPARγ and CCAAT/enhancer binding protein (C/EBP)β (Takahata et al., 2004). Paradoxically, decrease or knockout of MSTN leads to suppression of body fat accumulation and increaseof myogenesis (Lin et al., 2002; McPherron and Lee, 2002). Researchers have found that Mstn-knockout ($Mstn^{-/-}$) mice exhibit browning of white adipose tissues. The mechanism involved is that there are activated PGC1α and Fndc5 in $MSTN^{-/-}$ skeletal muscle in mice (Shan et al., 2013). C McFarlane et al also found that Mstn treated myoblasts inhibited Fndc5 to express, but MSTN inhibition promted Fndc5 levels in circulation and in muscles. $Mstn^{-/-}$ adipocytes showed enhanced Fndc5 expression. $Mstn^{-/-}$ adipocytes have improved mitochondrial function, increased mitochondria and heat production (Kong et al., 2018). Thus it can be seen that Fndc5 play an important role in MSTN regulating weight loss in mice. Studies have shown that Fndc5 overexpression enhanced energy expenditure, insulin sensitivity and lipolysis, and decreased hyperglyccemia, hyperlipidemia, hyperinsulinsm, norepinephrine levels and blood pressure in obese mice (Xiong et al., 2015). In our study, we also found an increase expression of Fndc5 in skeletal muscle, adipose tissue, differentiated C2C12 cells and 3T3-L1 cells.

To summarize, we demonstrate that Rb1 is a negenative regulator of obesity. Mice treated with Rb1 inhibited HFD-induced obesity, improved glucose intolerance, fat liver and adipose function. MSTN and Fndc5 were involved in this process. It is a potential therapeutic that Rb1 may be for treatment of obesity and obesity-related metabolic disorders (Fig6F).

Conclusions

Our results showed that Rb1 may ameliorate obesity in part through MSTN/Fndc5 signaling pathway. Our study provides important experimental evidences for the treatment of obesity by Rb1.

Abbreviations

Rb1: Ginsenoside Rb1; HFD: High-Fat Diet; MSTN：myostain；TG：triglycerides；CTR：control；IPGTT：intraperitoneal glucose tolerance test；DMEM：Dulbecco's Modified Eagles Medium；FBS：fetal bovine serum；ADV：adenovirus；MOI：multiplicity of infection；H&E：hematoxylin and eosin；epiWAT：epididymis white adipose tissue； subcutaneous white adipose tissue：ingWAT；；C/EBP：CCAAT/enhancer binding protein.

Declarations

Authors' contributions

LHS, KJY made substantial contributions to the conception. LGJ, WWJ LHD and WL implemented experiments. YXL and YWJ analyzed the data and made figures for this manuscript. ZWC QT and LXT wrote the original draft and substantively revised it. SYY administrated this project. SYY, ZWC and YWJ funded this experiment. All authors read and approved the final manuscript.

Funding

Funding sources: This work was assisted by the Shandong Key research and development program, China (2019GSF108276, 2019GSF108013, 2019GSF108055, 2019GSF108057, 2019GSF108242), advanced medical research institute project (22480089398409), the Taishan Scholar Project of Shandong Province of China (tsqn20161066), the Natural Science Foundation for Distinguished Young Scholars of Shandong Province (ZR2020JQ30), China Postdoctoral Science Foundation (2018M642673 and 2018M640638), National Natural Science Foundation of China (81800775, 81600344, 82071939), Shandong Provincial Natural Science Foundation, China (ZR2018BH010, ZR2016HQ29, ZR2020MH027).

Availability of data and materials

The datasets used or analyzed during the current study are available from

the corresponding author on reasonable request.

Ethics approval and consent to participate

This study was approved by the ethics committee of Qilu Hospital, Cheeloo

College of Medicine, Shandong University.

Consent for publication

Not applicable.

Competing interests

The authors declare that they have no competing interests.

Acknowledgements

Not applicable.

References

Algire, C., Medrikova, D., and Herzig, S. (2013). White and brown adipose stem cells: from signaling to clinical implications. *Biochim Biophys Acta* 1831(5)**,** 896-904. doi: 10.1016/j.bbalip.2012.10.001.

Baek, M.O., Ahn, C.B., Cho, H.J., Choi, J.Y., Son, K.H., and Yoon, M.S. (2019). Simulated microgravity inhibits C2C12 myogenesis via phospholipase D2-induced Akt/FOXO1 regulation. *Sci Rep* 9(1), 14910. doi: 10.1038/s41598-019-51410-7.

Bernardo, B.L., Wachtmann, T.S., Cosgrove, P.G., Kuhn, M., Opsahl, A.C., Judkins, K.M., et al. (2010). Postnatal PPAR delta Activation and Myostatin Inhibition Exert Distinct yet Complimentary Effects on the Metabolic Profile of Obese Insulin-Resistant Mice. *Plos One* 5(6). doi: 10.1371/journal.pone.0011307.

Chan, L.S., Yue, P.Y., Kok, T.W., Keung, M.H., Mak, N.K., and Wong, R.N. (2012). Ginsenoside-Rb1 promotes adipogenesis through regulation of PPARγ and microRNA-27b. *Horm Metab Res* 44(11), 819-824. doi: 10.1055/s-0032-1321909.

Duncan, R.E., Ahmadian, M., Jaworski, K., Sarkadi-Nagy, E., and Sul, H.S. (2007). Regulation of lipolysis in adipocytes. *Annu Rev Nutr* 27, 79-101. doi: 10.1146/annurev.nutr.27.061406.093734.

Faust, I.M., Johnson, P.R., Stern, J.S., and Hirsch, J. (1978). Diet-induced adipocyte number increase in adult rats: a new model of obesity. *Am J Physiol* 235(3), E279-286. doi: 10.1152/ajpendo.1978.235.3.E279.

Garcia-Fontana, B., Reyes-Garcia, R., Morales-Santana, S., Avila-Rubio, V., Munoz-Garach, A., Rozas-Moreno, P., et al. (2016). Relationship between myostatin and irisin in type 2 diabetes mellitus: a compensatory mechanism to an unfavourable metabolic state? *Endocrine* 52(1), 54-62. doi: 10.1007/s12020-015-0758-8.

Guo, R., Wang, L., Zeng, X., Liu, M., Zhou, P., Lu, H., et al. (2020). Aquaporin 7 involved in GINSENOSIDE-RB1-mediated anti-obesity via peroxisome proliferator-activated receptor gamma pathway. *Nutr Metab (Lond)* 17, 69. doi: 10.1186/s12986-020-00490-8.

Hibuse, T., Maeda, N., Nagasawa, A., and Funahashi, T. (2006). Aquaporins and glycerol metabolism. *Biochim Biophys Acta* 1758(8), 1004-1011. doi: 10.1016/j.bbamem.2006.01.008.

Hittel, D.S., Berggren, J.R., Shearer, J., Boyle, K., and Houmard, J.A. (2009). Increased Secretion and Expression of Myostatin in Skeletal Muscle From Extremely Obese Women. *Diabetes* 58(1), 30-38. doi: 10.2337/db08-0943.

Jeremic, N., Chaturvedi, P., and Tyagi, S.C. (2017). Browning of White Fat: Novel Insight Into Factors, Mechanisms, and Therapeutics. *J Cell Physiol* 232(1), 61-68. doi: 10.1002/jcp.25450.

Kim, J.H. (2018). Pharmacological and medical applications of Panax ginseng and ginsenosides: a review for use in cardiovascular diseases. *J Ginseng Res* 42(3), 264-269. doi: 10.1016/j.jgr.2017.10.004.

Kong, X., Yao, T., Zhou, P., Kazak, L., Tenen, D., Lyubetskaya, A., et al. (2018). Brown Adipose Tissue Controls Skeletal Muscle Function via the Secretion of Myostatin. *Cell Metab* 28(4), 631-643.e633. doi: 10.1016/j.cmet.2018.07.004.

Kopelman, P.G. (2000). Obesity as a medical problem. *Nature* 404(6778), 635-643. doi: 10.1038/35007508.

Langley, B., Thomas, M., Bishop, A., Sharma, M., Gilmour, S., and Kambadur, R. (2002). Myostatin inhibits myoblast differentiation by down-regulating MyoD expression. *Journal of Biological Chemistry* 277(51), 49831-49840. doi: 10.1074/jbc.M204291200.

Lebrasseur, N.K. (2012). Building muscle, browning fat and preventing obesity by inhibiting myostatin. *Diabetologia* 55(1), 13-17. doi: 10.1007/s00125-011-2361-8.

Lim, S., Park, J., and Um, J.Y. (2019). Ginsenoside Rb1 Induces Beta 3 Adrenergic Receptor-Dependent Lipolysis and Thermogenesis in 3T3-L1 Adipocytes and db/db Mice. *Front Pharmacol* 10, 1154. doi: 10.3389/fphar.2019.01154.

Lin, J., Arnold, H.B., Della-Fera, M.A., Azain, M.J., Hartzell, D.L., and Baile, C.A. (2002). Myostatin knockout in mice increases myogenesis and decreases adipogenesis. *Biochem Biophys Res Commun* 291(3), 701-706. doi: 10.1006/bbrc.2002.6500.

Lyons, J.A., Haring, J.S., and Biga, P.R. (2010). Myostatin expression, lymphocyte population, and potential cytokine production correlate with predisposition to high-fat diet induced obesity in mice. *PLoS One* 5(9), e12928. doi: 10.1371/journal.pone.0012928.

McPherron, A.C., Lawler, A.M., and Lee, S.J. (1997). Regulation of skeletal muscle mass in mice by a new TGF-beta superfamily member. *Nature* 387(6628), 83-90. doi: 10.1038/387083a0.

McPherron, A.C., and Lee, S.J. (1997). Double muscling in cattle due to mutations in the myostatin gene. *Proceedings of the National Academy of Sciences of the United States of America* 94(23), 12457-12461. doi: 10.1073/pnas.94.23.12457.

McPherron, A.C., and Lee, S.J. (2002). Suppression of body fat accumulation in myostatin-deficient mice. *J Clin Invest* 109(5), 595-601. doi: 10.1172/JCI13562.

Milan, G., Dalla Nora, E., Pilon, C., Pagano, C., Granzotto, M., Manco, M., et al. (2004). Changes in muscle myostatin expression in obese subjects after weight loss. *J Clin Endocrinol Metab* 89(6), 2724-2727. doi: 10.1210/jc.2003-032047.

Park, S., Ahn, I.S., Kwon, D.Y., Ko, B.S., and Jun, W.K. (2008). Ginsenosides Rb1 and Rg1 suppress triglyceride accumulation in 3T3-L1 adipocytes and enhance beta-cell insulin secretion and viability in Min6 cells via PKA-dependent pathways. *Biosci Biotechnol Biochem* 72(11), 2815-2823. doi: 10.1271/bbb.80205.

Prudente, S., Flex, E., Morini, E., Turchi, F., Capponi, D., De Cosmo, S., et al. (2007). A functional variant of the adipocyte glycerol channel aquaporin 7 gene is associated with obesity and related metabolic abnormalities. *Diabetes* 56(5), 1468-1474. doi: 10.2337/db06-1389.

Shan, T., Liang, X., Bi, P., and Kuang, S. (2013). Myostatin knockout drives browning of white adipose tissue through activating the AMPK-PGC1α-Fndc5 pathway in muscle. *Faseb j* 27(5), 1981-1989. doi: 10.1096/fj.12-225755.

Shang, W., Yang, Y., Jiang, B., Jin, H., Zhou, L., Liu, S., et al. (2007). Ginsenoside Rb1 promotes adipogenesis in 3T3-L1 cells by enhancing PPARgamma2 and C/EBPalpha gene expression. *Life Sci* 80(7), 618-625. doi: 10.1016/j.lfs.2006.10.021.

Shang, W., Yang, Y., Zhou, L., Jiang, B., Jin, H., and Chen, M. (2008). Ginsenoside Rb1 stimulates glucose uptake through insulin-like signaling pathway in 3T3-L1 adipocytes. *J Endocrinol* 198(3), 561-569. doi: 10.1677/joe-08-0104.

Shen, L., Xiong, Y., Wang, D.Q., Howles, P., Basford, J.E., Wang, J., et al. (2013). Ginsenoside Rb1 reduces fatty liver by activating AMP-activated protein kinase in obese rats. *J Lipid Res* 54(5), 1430-1438. doi: 10.1194/jlr.M035907.

Shin, S.S., and Yoon, M. (2018). Korean red ginseng (Panax ginseng) inhibits obesity and improves lipid metabolism in high fat diet-fed castrated mice. *J Ethnopharmacol* 210, 80-87. doi: 10.1016/j.jep.2017.08.032.

Song, B., Sun, Y., Chu, Y., Wang, J., Zheng, H., Liu, L., et al. (2020). Ginsenoside Rb1 Alleviated High-Fat-Diet-Induced Hepatocytic Apoptosis via Peroxisome Proliferator-Activated Receptor γ. *Biomed Res Int* 2020, 2315230. doi: 10.1155/2020/2315230.

Takahata, T., Kumano, T., Ookawa, K., Hayakari, M., Kakizaki, I., and Tsuchida, S. (2004). Inhibition of 3T3-L1 adipocyte differentiation by 6-ethoxyzolamide: repressed peroxisome proliferator-activated receptor gamma mRNA and enhanced CCAAT/enhancer binding protein beta mRNA levels. *Biochem Pharmacol* 67(9), 1667-1675. doi: 10.1016/j.bcp.2003.12.039.

Wang, H., Reaves, L.A., and Edens, N.K. (2006). Ginseng extract inhibits lipolysis in rat adipocytes in vitro by activating phosphodiesterase 4. *J Nutr* 136(2), 337-342. doi: 10.1093/jn/136.2.337.

Wu, Y., Huang, X.F., Bell, C., and Yu, Y. (2018). Ginsenoside Rb1 improves leptin sensitivity in the prefrontal cortex in obese mice. *CNS Neurosci Ther* 24(2), 98-107. doi: 10.1111/cns.12776.

Xiong, X.Q., Chen, D., Sun, H.J., Ding, L., Wang, J.J., Chen, Q., et al. (2015). FNDC5 overexpression and irisin ameliorate glucose/lipid metabolic derangements and enhance lipolysis in obesity. *Biochim Biophys Acta* 1852(9), 1867-1875. doi: 10.1016/j.bbadis.2015.06.017.

Xiong, Y., Shen, L., Liu, K.J., Tso, P., Xiong, Y., Wang, G., et al. (2010). Antiobesity and antihyperglycemic effects of ginsenoside Rb1 in rats. *Diabetes* 59(10), 2505-2512. doi: 10.2337/db10-0315.

Yu, X., Ye, L., Zhang, H., Zhao, J., Wang, G., Guo, C., et al. (2015). Ginsenoside Rb1 ameliorates liver fat accumulation by upregulating perilipin expression in adipose tissue of db/db obese mice. *J Ginseng Res*

39(3), 199-205. doi: 10.1016/j.jgr.2014.11.004.

Zhang, C., McFarlane, C., Lokireddy, S., Masuda, S., Ge, X., Gluckman, P.D., et al. (2012). Inhibition of myostatin protects against diet-induced obesity by enhancing fatty acid oxidation and promoting a brown adipose phenotype in mice. *Diabetologia* 55(1), 183-193. doi: 10.1007/s00125-011-2304-4.

Figures

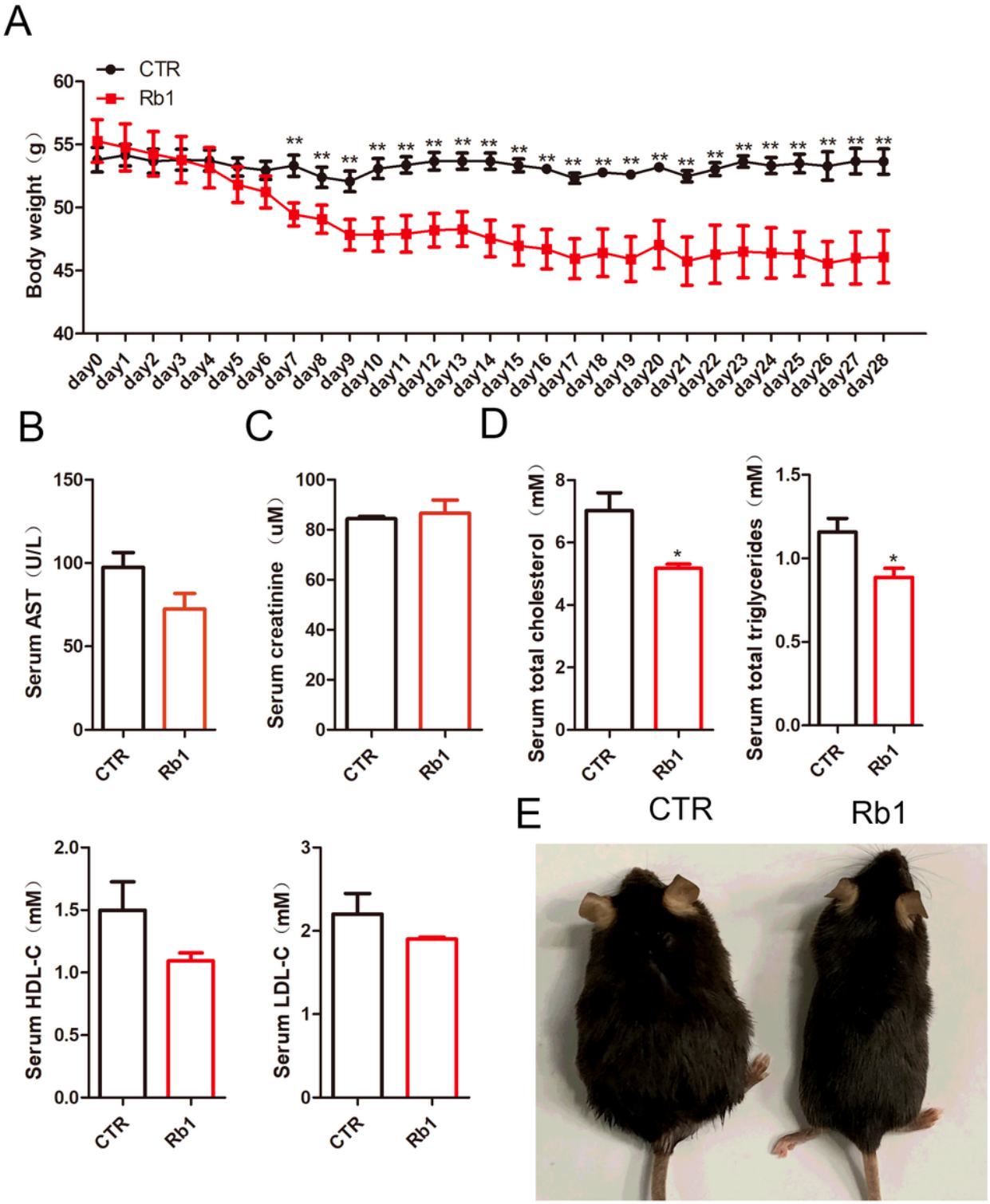

Figure 1

Effect of Rb1 in body weight, cholesterol and triglyceride in obese mice. A. Variations of the mouse body weight from the two groups. B. The serum levels of AST, C. creatinine, D. TC, TG, HDL-C and LDL-C. E. Representative mouse photographs in two groups. *p< 0.05 VS CTR group, **p< 0.01 VS CTR group.n=5.

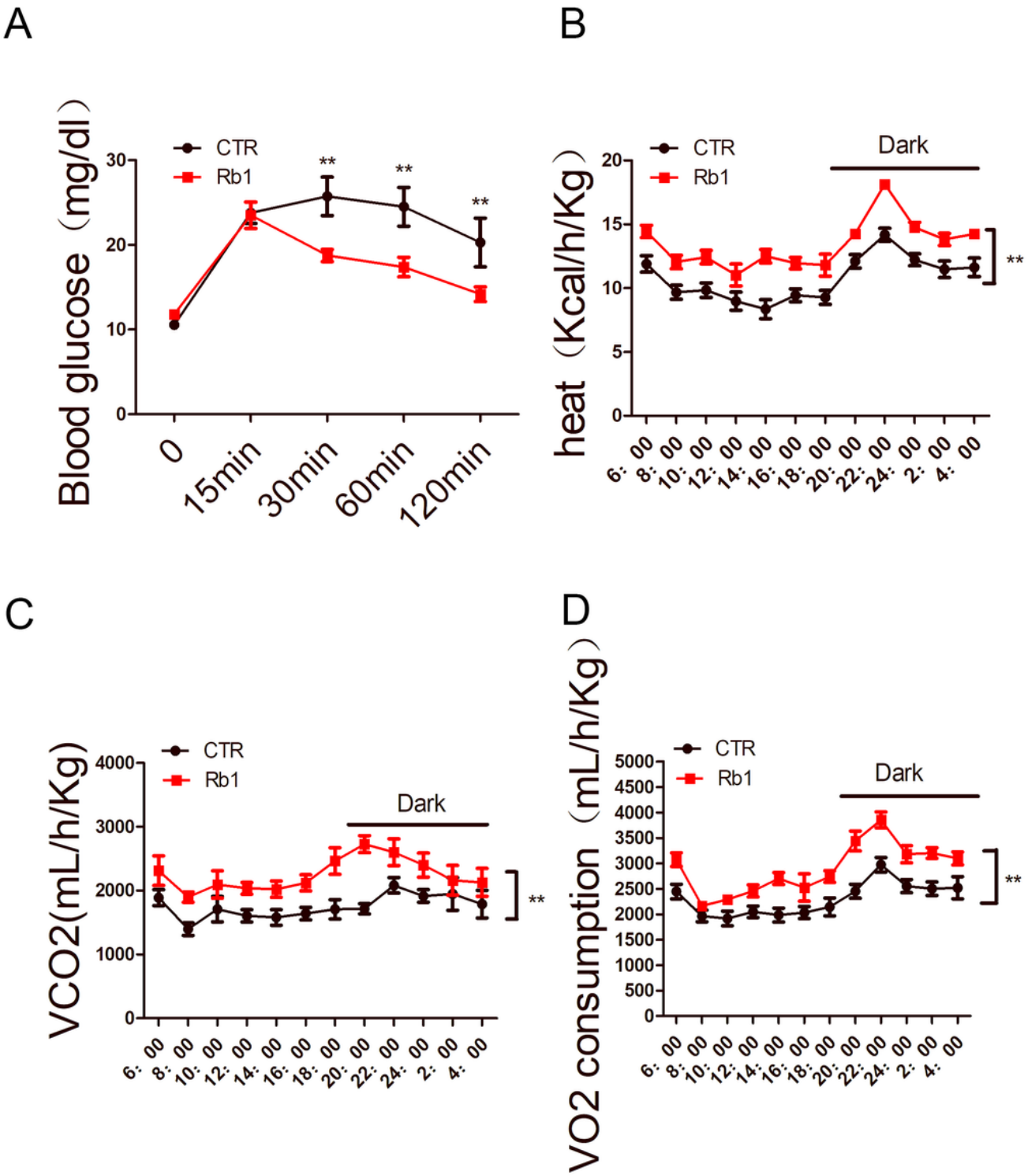

Figure 2

Effect of Rb1 on glucose tolerance and metabolism. A. Glucose tolerance test. B. Heat production. C. The carbon dioxide production D. The oxygen consumption. **p< 0.01 VS CTR group.n=5.

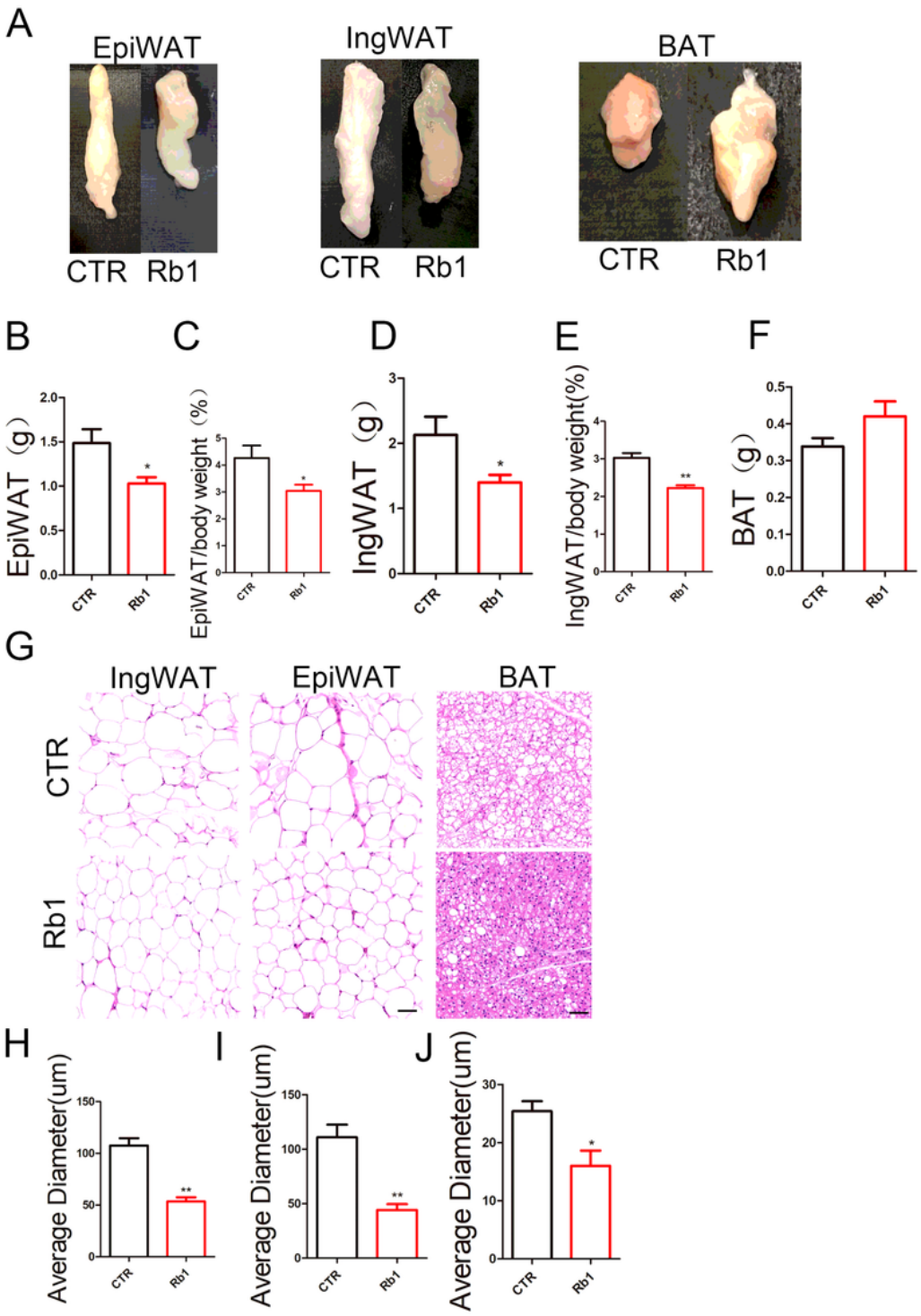

Figure 3

Effect of Rb1 on adipocyte hypertrophy and fatty liver. A. Representative photographs of EpiWAT, IngWAT, BAT. B. Quantification of EpiWAT. C. Quantification of EpiWAT/body weight. D. Quantification of IngWAT. E. Quantification of IngWAT/ body weight. F. Quantification of BAT. G. Representative HE images of EpiWAT, IngWAT and BAT in two group of mice. H. Quantification of average IngWAT diameters. I.

Quantification of average EpiWAT diameters. J. Quantification of average BAT diameters. scale bar=50μm. n=5. *p< 0.05 VS CTR group, **p< 0.01 VS CTR group.

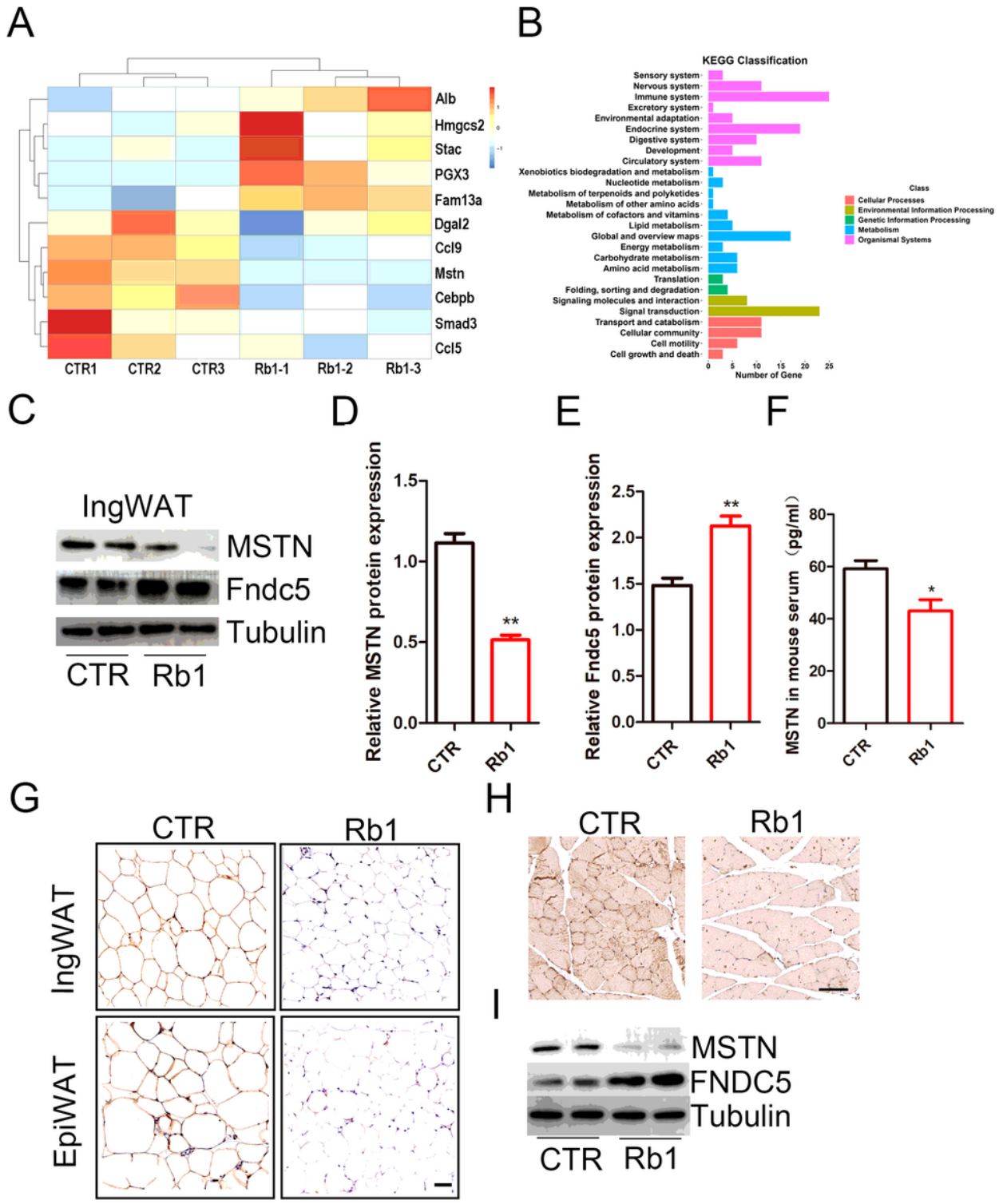

Figure 4

Effect of Rb1 on MSTN expression in adipose tissue. A. The representative genes with >1.5-fold upregulation or >1.5-fold downregulation in CTR and Rb1 mouse adipose tissue. n=3. B. The signaling pathways of Rb1 regulates genes involved in. C. Protein expression of MSTN and Fndc5 in adipose

tissue. n=3. D. Quantification of relative MSTN protein expression. E. Quantification of relative Fndc5 protein expression. F. The MSTN in mouse serum. n=5. G. Immunohistochemical staining showed the expression of MSTN in EpiWAT and IngWAT. n=5. H. Representative photograph of MSTN expression in CTR and Rb1 mouse skeletal muscle. I. Western blot analysis of MSTN and Fndc5 protein expression in mouse skeletal muscle. n=3. J. *p< 0.05 VS CTR group, **p< 0.01 VS CTR group.

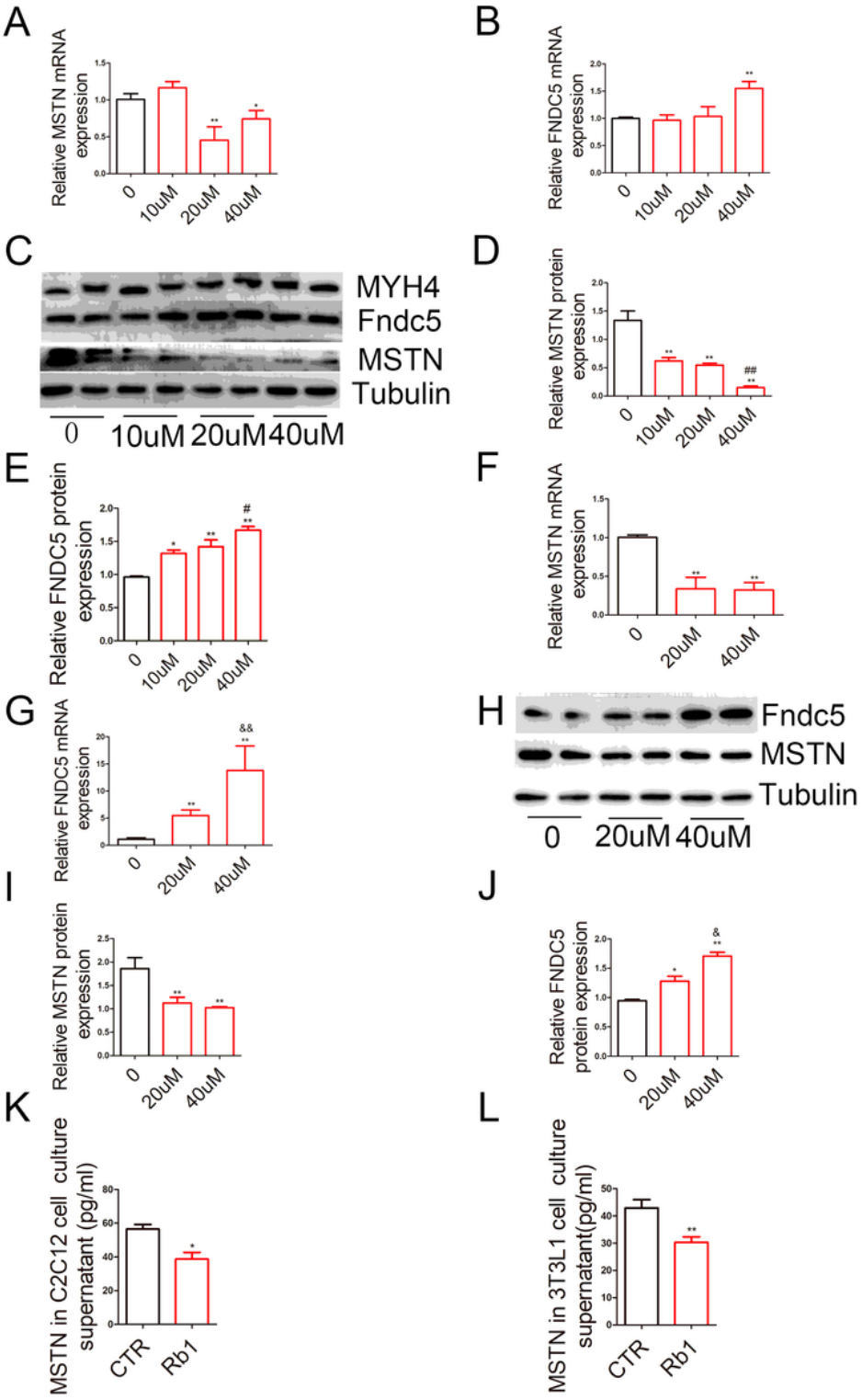

Figure 5

Rb1 regulates MSTN and Fndc5 mRNA and protein expression in differentiated C2C12 myoblasts and 3T3-L1 adipocytes. A-B. The effect of 0, 10μM, 20μM, 40μM Rb1 on MSTN and Fndc5 mRNA expression in differentiated C2C12 myoblasts. C. Western blot analysis of MYH4, MSTN, Fndc5 expression in differentiated C2C12 myoblasts. D-E. Statistical analysis of MSTN and Fndc5 protein level. F-G. The effect of 0, 20μM, 40μM Rb1 on MSTN and Fndc5 mRNA expression in differentiated 3T3-L1 adipocytes. H. Western blot analysis of MSTN, Fndc5 expression in differentiated 3T3-L1 adipocytes. I-J. Statistical analysis of MSTN and Fndc5 protein level. K. The MSTN expression in culture supernatant of differentiated C2C12 myoblasts. L. The MSTN expression in culture supernatant of differentiated 3T3-L1 adipocytes. n=5. *p< 0.05 VS CTR group, **p< 0.01 VS CTR group, # p< 0.05 VS 10μM Rb1, ## p<0.01 VS 10μM Rb1, & p< 0.05 VS 20μM Rb1, && p<0.01 VS 20μM Rb1.

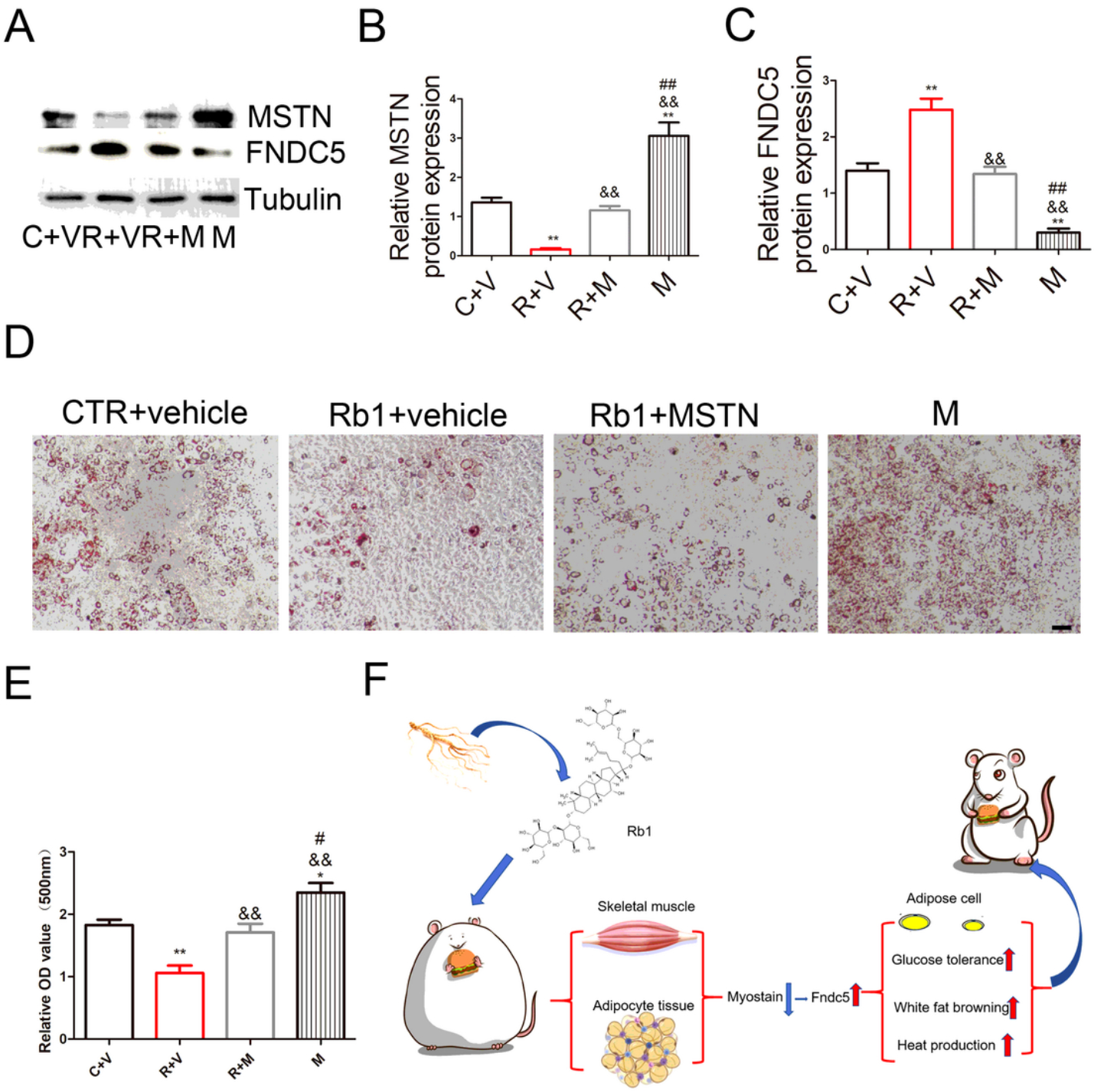

Figure 6

Rb1 inhibit lipid deposit through MSTN in 3T3-L1 induced adipocytes. A. WB analysis of MSTN and Fndc5 expression. B-C. Statistical analysis of A. D. Representative Oil red O staining. E. Statistical analysis of D. scale bar=50μm. F. Schematic diagram about the mechanism of Rb1 in adipose tissue and obesity. n=5. **p< 0.01 VS C+V group, &&p< 0.01 VS R+V group.## p< 0.01 VS R+M group.

Supplementary Files

This is a list of supplementary files associated with this preprint. Click to download.

- s1.png